Dynamical effects of softening in N-body simulations of disc galaxies

Method and first applications

Alessandro B. Romeo

Onsala Space Observatory, Chalmers University of Technology, S-43992 Onsala, Sweden (romeo@oso.chalmers.se)

Abstract. Two questions that naturally arise in N-body simulations of stellar systems are:

1. How can we compare experiments that employ different types of softened gravity?
2. Given a particular type of softened gravity, which choices of the softening length optimize the faithfulness of the experiments to the Newtonian dynamics?

We devise a method for exploring the dynamical effects of softening, which provides detailed answers in the case of 2-D simulations of disc galaxies and also solves important aspects of the 3-D problem. In the present paper we focus on two applications that reveal the dynamical differences between the most representative types of softened gravity, including certain anisotropic alternatives. Our method is potentially important not only for testing but also for developing new ideas about softening. Indeed, it opens a *direct* route to the discovery of optimal types of softened gravity for given dynamical requirements, and thus to the accomplishment of a physically consistent modelling.

Key words: gravitation – methods: analytical – methods: numerical – galaxies: kinematics and dynamics – galaxies: spiral – stellar dynamics

1. Introduction

In N-body simulations of stellar systems the gravitational interaction is modified for curing the Newtonian divergence at short distances. Basically, such modifications are introduced through a soft cut-off: the softening length s. However, the precise form in which they are implemented can vary. Since gravity plays a fundamental role in these systems and the gravitational interaction is modified precisely where it becomes singular, the dynamical effects of softening should be well understood when designing experiments and interpreting their results. This dynamical problem has recently stimulated considerable

interest (e.g., Hernquist & Barnes 1990; Hernquist & Ostriker 1992; Kandrup et al. 1992; Pfenniger 1993; Pfenniger & Friedli 1993; Gurzadyan & Pfenniger 1994; Romeo 1994, hereafter Paper I; Byrd 1995; Gerber 1996; Merritt 1996; Weinberg 1996; Sommer-Larsen et al. 1997; Theis 1997; see also Goodman et al. 1993; Farouki & Salpeter 1994). For extensive overviews see the above-mentioned Pfenniger & Friedli (1993), Gurzadyan & Pfenniger (1994) and Paper I.

In Paper I we have investigated the stability problem in the case of 2-D models with Plummer softening, which are commonly employed in simulations of disc galaxies. The basic message is that the effect of softening becomes strongly artificial for $s \gtrsim \lambda/2\pi$, λ being the typical radial wavelength, which means half an order of magnitude below the expected value. The major results are summarized in the form of a criterion of approximate physical consistency for s and a stability criterion for the Toomre parameter. (Other important aspects of the stability problem have been considered by Byrd 1995.)

In the present paper we carry out five extensions, as is discussed below.

1. We generalize the stability analysis of Paper I to an *arbitrary* isotropic form of softening. This is a natural extension since types of softened gravity different from the standard Plummer softening are becoming more and more commonly employed (e.g., Combes et al. 1990; Palouš et al. 1993; Shlosman & Noguchi 1993). In particular, the alternatives proposed by Hernquist & Katz (1989) and Pfenniger & Friedli (1993) reflect an interesting idea, viz. that softening should be as localized as possible since there is no clear reason for modifying the gravitational interaction at long distances, and it is tempting to explore its dynamical consequences. From a more general point of view, this and the following extensions provide the tools for comparing experiments that employ different types of softened gravity.
2. We investigate the implications of our stability analysis for the classical relaxation problem (Rybicki 1972; White

1988). Relaxation and stability[1] are intimately related in self-gravitating systems, and even simple treatments reveal their strong coupling through random motions. On the other hand, the contribution of velocity dispersion to the relaxation time has been understood only in part and, because of that, the classical argument favouring the choice of large values of s is wrong. We revise this argument and conclude that neither small nor large values of s are convenient. Surprisingly, there exists an intermediate choice of s that *optimizes* the 'dynamical resolution' of the model, i.e. its faithfulness in simulating the dynamics of 3-D discs with Newtonian gravity, especially in situations near to the stability threshold. We identify the optimal characteristics, and show how to evaluate them for a given type of softened gravity. In addition to investigating this aspect of the relaxation problem, we explain how effectively softening reduces noise on various scales.

3. We complete the examination of 2-D models with isotropic softening by investigating the equilibrium problem for an axisymmetric state with epicyclic motions. In particular, we explain how significantly the circular speed and related quantities deviate from their Newtonian behaviours at various distances from the centre.

4. We consider 3-D models with isotropic softening and examine two limiting cases: discs and the simple, yet instructive, Jeans problem. An extension to 3D has been encouraged by Friedli (1994) and Junqueira & Combes (1996, see the interesting remarks in Sect. 2.2). Real stellar systems have several gravitationally interacting components. Both N-body simulations and theoretical works are forced to use simplified models, which do not necessarily provide faithful representations of the complexity of such systems. Our motivation is to understand the basic differences between the dynamical effects of softening in 3D and 2D, in the presence of a single stellar component (3-D vs. 2-D discs and Jeans problem vs. discs). In particular, we point up the *strong* modifications introduced by a homogeneous geometry and the absence of rotation.

5. We complete the examination of 3-D models by discussing the basic dynamical effects of softening anisotropy. The idea underlying this extension is that softening should be anisotropic in simulations of stellar systems where significantly higher spatial resolution is required along a certain direction, such as in disc galaxies. The alternative family of softening recently proposed by Pfenniger & Friedli (1993) reflects such an important idea, and it is tempting to explore the dynamical relations between its members. (An analogous idea has been discussed in the context of smoothed particle hydrodynamics by Shapiro et al. 1994, 1996 and Fulbright et al. 1995; Hernquist, private communication, has remarked that in models with anisotropic smoothing there

may be a significant tendency for angular momentum not to be conserved.)

These extensions all together form a method for exploring the dynamical effects of softening in N-body simulations of stellar systems. Our method is described in Sect. 2, and is structured as in the previous discussion. The two applications mentioned in the same context are shown in Sect. 3 (see also Appendix A). The conclusions of this paper are drawn in Sect. 4, where we present our contribution in a more general perspective and motivate future applications.

2. Method

2.1. 2-D models with isotropic softening

2.1.1. Stability

In 2-D discs with isotropic softened gravity, a given surface-density perturbation $\Sigma_1(\boldsymbol{R}, t)$ induces a potential perturbation

$$\Phi_1(\boldsymbol{R}, t) = -G \int \varphi_s(|\boldsymbol{R} - \boldsymbol{R}'|)\,\Sigma_1(\boldsymbol{R}', t)\,\mathrm{d}^2\boldsymbol{R}'\,, \tag{1}$$

where $-Gm\varphi_s(R)$ is the point-mass potential, which depends on the softening length s [$\varphi_s(R)$ is also known as the softening kernel]. In analysing the Poisson equation (1), we adopt the lowest-order WKBJ approach, as in Paper I, but with a different albeit asymptotically equivalent spectral representation. In simple terms, the new feature consists in considering perturbations with a radial dependence $g_1(R) = \tilde{g}_1\,\mathrm{J}_0(kR)$ rather than $g_1(R) = \hat{g}_1\,\mathrm{e}^{ikR}$, where k is the radial wavenumber and J_ν denotes the Bessel function of the first kind and order ν (see, e.g., Abramowitz & Stegun 1972). The Bessel-Hankel representation is more convenient than the Fourier representation because it allows factorizing the convolution in the Poisson equation directly, without any assumption on the form of $\varphi_s(R)$:

$$\tilde{\Phi}_1 = -2\pi G\,\mathscr{H}_0[\varphi_s(R)](k)\,\tilde{\Sigma}_1\,, \tag{2}$$

where $\mathscr{H}_\nu$ denotes the Hankel transform of order ν (see, e.g., Sneddon 1972; Bracewell 1986):

$$\mathscr{H}_\nu[g(R)](k) = \int_0^\infty g(R)\,\mathrm{J}_\nu(kR)\,R\,\mathrm{d}R\,. \tag{3}$$

The reduction factor. Equation (2) admits of a simple interpretation: the potential perturbation induced by a given surface-density perturbation is weakened by a factor

$$\mathscr{S} \equiv \frac{\mathscr{H}_0[\varphi_s(R)](k)}{\mathscr{H}_0[\varphi_\mathrm{N}(R)](k)}\,, \tag{4}$$

$-Gm\varphi_\mathrm{N}(R)$ being the Newtonian point-mass potential. Correspondingly, the contribution of self-gravity to the dispersion relation is weakened through a reduction of the active unperturbed surface density by the same factor. Thus, $\mathscr{S}$ provides complete information about the effect of isotropic softening on the stability of 2-D discs, and its evaluation is the starting-point

---

[1]   In this and similar contexts, 'stability' should be understood in the general sense of 'stability properties'; it is not implied that the system is stable. The same applies to the use of 'relaxation' and 'equilibrium'.

of our method. There are two complementary routes to $\mathscr{S}$. One is to calculate it analytically from:

$$\mathscr{S}(|k|s) = |k| \, \mathscr{H}_0[\varphi_s(R)](k) \tag{5}$$

(use, e.g., the comprehensive table of integrals by Gradshteyn & Ryzhik 1994). This equation follows directly from Eq. (4), being $\varphi_N(R) = 1/R$ and $\mathscr{H}_0[1/R](k) = 1/|k|$. The other is to compute it numerically from:

$$\mathscr{S}(|k|s) = 1 - \mathscr{H}_1\left[\frac{1}{R^2} - f_s(R)\right](|k|) , \tag{6}$$

$-Gm^2 f_s(R)$ being the point-mass force (use, e.g., the extensive and well-documented NAG library; for algorithms of fast Hankel transform see, e.g., Gueron 1994; van Veldhuizen et al. 1994). This equation is more convenient than the original Eq. (5) because the slow decay of the oscillatory integrand as $R \to \infty$ is speeded up. Such an improvement is obtained with simple tricks, viz. integrating by parts and singling out the Newtonian behaviour of $f_s(R)$ at long distances.

The effective scale height. Once $\mathscr{S}(|k|s)$ has been evaluated, the second step is to analyse its behaviour at small $|k|s$ since stability is basically a large-scale property. In order to understand the general features of this behaviour, we can equivalently start from Eq. (5) or (6) and use techniques of asymptotic expansion of integrals (see, e.g., Bender & Orszag 1978). In Eq. (5), we should first single out the Newtonian $1/R$-dependence of $\varphi_s(R)$ at long distances, and then expand $J_0(kR)$. In Eq. (6), we can directly expand $J_1(|k|R)$. The result is that $\mathscr{S} \sim 1 - |k|h$, where in each case

$$h = \int_0^\infty [1 - R\varphi_s(R)]\,\mathrm{d}R = \frac{1}{2}\int_0^\infty [1 - R^2 f_s(R)]\,\mathrm{d}R . \tag{7}$$

This quantity is positive in types of softened gravity of practical interest, and has an important dynamical meaning. In fact, a comparison with the reduction factor of 3-D discs with Newtonian gravity (Shu 1968; Vandervoort 1970; Romeo 1992) shows that softening mimics thickness on large scales and h has the effect of a scale height, as far as density waves are concerned (for bending waves see Masset & Tagger 1996). As an alternative to Eq. (7), h can be evaluated from the conversion factor

$$\frac{h}{s} = -\mathscr{S}'(|k|s = 0) . \tag{8}$$

Characteristics. The third and last step is to extract detailed information concerning the stability properties. This part of the method has been described in Paper I and can be generalized without special difficulties. So in the following discussion we briefly introduce the basic concepts and point out the major results of the stability analysis. We adopt the basic fluid description with the following scaling and parametrization:

$$\bar{\lambda} \equiv \frac{\lambda}{\lambda_T} , \quad \text{where} \quad \lambda_T = \frac{2\pi}{k_T} \equiv \frac{4\pi^2 G\Sigma}{\kappa^2} , \tag{9}$$

$$Q \equiv \frac{c\kappa}{\pi G\Sigma} \quad \text{(Safronov-Toomre parameter)} , \tag{10}$$

$$\eta \equiv sk_T \quad \text{(softening parameter)} , \tag{11}$$

$$\zeta \equiv hk_T \quad \text{(effective thickness parameter)} , \tag{12}$$

where λ is the radial wavelength of the perturbation, λ_T is the Toomre wavelength, Σ is the unperturbed surface density, κ is the epicyclic frequency and c is the planar sound speed. The stability properties are described by the marginal stability curve, i.e. the dispersion relation for marginally stable perturbations viewed as a curve in the $(\bar{\lambda}, Q^2)$ plane for a given η:

$$Q^2 + 4\bar{\lambda}\left[\bar{\lambda} - \mathscr{S}(\eta/\bar{\lambda})\right] = 0 . \tag{13}$$

In particular, the stability level is measured by the effective parameter

$$Q_{\mathrm{eff}} = \frac{Q}{\bar{Q}(\eta)} , \tag{14}$$

where the threshold $\bar{Q}(\eta)$ corresponds to the square root of the global maximum of the marginal curve, and the typical radial wavelength corresponds to the location $\bar{\lambda}_{\max}(\eta)$ of this maximum. The values of η and the related quantities that characterize the stability properties are presented below.

- The conversion factor $\zeta/\eta = -\mathscr{S}'(\eta/\bar{\lambda} = 0)$, now expressed in dimensionless form, has already been discussed (cf. the effective scale height).
- The safety threshold for approximate physical consistency is $\eta_{\mathrm{safe}} = \frac{1}{5}(\zeta/\eta)^{-1}$. For $\eta \lesssim \eta_{\mathrm{safe}}$, i.e. $\zeta \lesssim \frac{1}{5}$, softening mimics the effect of thickness. In particular, $\bar{Q} \approx 1 - 2\zeta$ and $\bar{\lambda}_{\max} \simeq \frac{1}{2}$. For $\eta \gtrsim \eta_{\mathrm{safe}}$, softening causes artificial stabilization and a moderate degree of 'blueshift'.
- The critical value η_{crit} is such that $\bar{Q}(\eta_{\mathrm{crit}}) = 0$. For $\eta \geq \eta_{\mathrm{crit}}$, the fundamental meaning of velocity dispersion becomes *obscure* because the stability level is no longer actively controlled by Q_{eff}. This fact has serious dynamical implications: it artificially precludes the possibility of simulating regimes of normal spiral structure, which require fine-tuned choices of the stability level.
- The critical radial wavelength is $\bar{\lambda}_{\mathrm{crit}} = \bar{\lambda}_{\max}(\eta_{\mathrm{crit}})$. Its deviation from $\bar{\lambda}_{\max}(0) = \frac{1}{2}$ indicates the sensitivity of $\bar{\lambda}_{\max}(\eta)$ for $\eta < \eta_{\mathrm{crit}}$.

2.1.2. Relaxation vs. stability

Let us investigate the implications of our stability analysis for the classical relaxation problem (Rybicki 1972; White 1988; see also Hockney & Eastwood 1988). We first sketch the basic ideas. The Rybicki-White relaxation time t_{RW} is proportional to the softening length s, the cube of velocity dispersion σ and the number of computer particles N. In turn, σ is proportional to the Safronov-Toomre parameter Q. So it seems that large values of s are convenient, since they result in a long t_{RW} for given Q and N. The idea underlying this argument is that a given Q corresponds to a constant stability level as s varies. But it is not so. In fact,
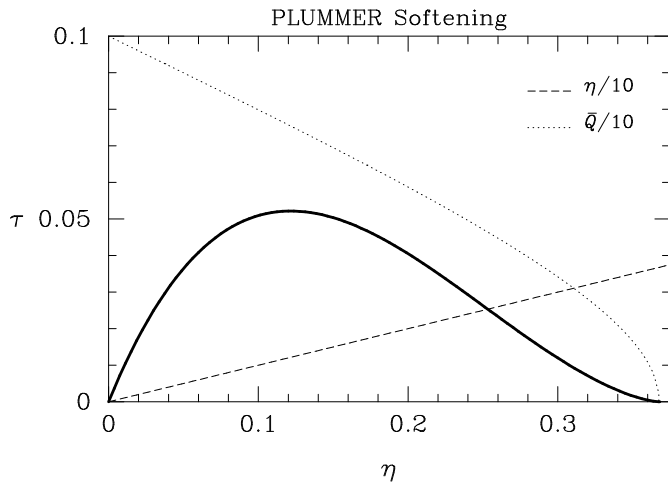
Fig. 1. The relaxation level $\tau(\eta) = \eta\,\bar{Q}^3(\eta)$ of 2-D discs with Plummer softened gravity, where η is the softening parameter and $\bar{Q}(\eta)$ is the stability threshold. The contribution of $\bar{Q}$ to the η-dependence of τ has major dynamical implications, as is pointed up in Sect. 2.1.2

the stability threshold $\bar{Q}$ depends on s and the level is measured by the effective parameter $Q_{\mathrm{eff}} = Q/\bar{Q}$. Thus large values of s are not convenient at all, because they correspond to a low $\bar{Q}$ and result in a short t_{RW} for given Q_{eff} and N. Furthermore, if t_{RW} is short for both small and large values of s, there must exist an intermediate choice of s that maximizes t_{RW}. Does it satisfy the criterion of approximate physical consistency? The answer is: Yes, it does. The identification of the optimal characteristics of 2-D discs with isotropic softened gravity is the focal point of our method.

The corrected Rybicki-White relaxation time. Originally, t_{RW} was derived by adopting a simple two-body treatment, and assuming that $f_s(R)$ is of the type: $f_s(R) = 0$ for $R \leq s$, $f_s(R) = 1/R^2$ for $R > s$. A generalization of t_{RW} to an arbitrary isotropic $f_s(R)$ is easy to derive and useful for comparing the effects of different types of softened gravity. The resulting t_{RW} is equal to the original one multiplied by a correction factor $\mathscr{C}$, which is one of the relaxation characteristics. Referring to the introductory discussion, we express t_{RW} in a form that splits the various contributions:

$$t_{\mathrm{RW}} = \mathscr{C} \cdot \tau(\eta)\, Q_{\mathrm{eff}}^3\, N \left(\frac{2\pi^3 G^2 \Sigma^3}{\kappa^5 M_{\mathrm{d}}} \right), \tag{15}$$

$$\mathscr{C}s = \left\{ \int_0^\infty [b f_s(b)]^2\, \mathrm{d}b \right\}^{-1}, \tag{16}$$

$$\tau(\eta) = \eta\, \bar{Q}^3(\eta), \tag{17}$$

where $\tau(\eta)$ measures the 'relaxation level' as η varies, M_{d} is the disc mass and b is the impact parameter. In addition, the original unspecified σ is interpreted as the radial velocity dispersion c (different specifications would only modify the proportionality factor).

Optimal characteristics. We now identify the values of η and the related quantities that optimize the relaxation and stability properties. Fig. 1 shows the behaviour of $\tau(\eta)$ in the case of Plummer softening, but the following discussion is general.

- The optimal relaxation level τ_{op} and the optimal choice η_{op} are such that $\tau_{\mathrm{op}} = \tau(\eta_{\mathrm{op}}) = \max\{\tau(\eta)\}$. The simple analytical approximation $\eta_{\mathrm{op}} \approx \frac{1}{8}(\zeta/\eta)^{-1}$ shows that $\eta_{\mathrm{op}} < \eta_{\mathrm{safe}}$.
- In 3-D discs with Newtonian gravity, the temperature anisotropy corresponding to the stability threshold for the optimal value $\zeta_{\mathrm{op}} \approx \frac{1}{8}$ would be $\delta_{\mathrm{op}} \approx \frac{2}{5}$, which means a *realistic* vertical-to-radial velocity dispersion ratio $c_z/c \approx 0.6$ [cf. Paper I, Eq. (16) and Fig. 3].
- The values η_{op1} and η_{op2} such that, e.g., $\tau(\eta_{\mathrm{op1}}) = \tau(\eta_{\mathrm{op2}}) = \frac{1}{2}\tau_{\mathrm{op}}$ specify a range of convenient choices of η, $\eta_{\mathrm{op1}} \lesssim \eta \lesssim \eta_{\mathrm{op2}}$, and complete the information concerning the optimal characteristics. The suggested definition is natural and especially meaningful because it turns out that $\eta_{\mathrm{op2}} \sim \eta_{\mathrm{safe}}$.

What about the reduction factor? A delicate aspect of the relaxation problem that has not been considered in the previous discussion concerns the effects of collective interactions between particles and self-consistent fluctuations on the dynamical evolution of the system (e.g., Romeo 1990 and references therein; Weinberg 1993; Zhang 1996). A thorough treatment of collective effects would demand titanic efforts even in simpler models (cf. Weinberg 1993). On the other hand, useful information is already contained in $\mathscr{S}(|k|s)$ since the diffusion properties are determined by the dispersion relation. In particular, the behaviour of $\mathscr{S}(|k|s)$ at large $|k|s$ ($\mathscr{S} \ll 1$) shows how effectively softening suppresses small-scale fluctuations, which represent an important source of noise in 2-D models (cf. White 1988; Schroeder & Comins 1989).

2.1.3. Equilibrium

The reduction factor. The equilibrium problem for an axisymmetric state with epicyclic motions can be solved by using the technique of Hankel transforms, which has already been introduced in the stability analysis. The basic idea is to $\mathscr{H}_0$-transform the Poisson equation twice: once for factorizing the convolution of $\varphi_s(R)$ and $\Sigma(R)$, and the other time for recovering $\Phi(R)$ [or, in the inverse problem, $\Sigma(R)$] from its transform. This is a natural generalization of the approach adopted by Toomre (1963) in the case with Newtonian gravity, where the Poisson equation can be expressed in differential form (see also Binney & Tremaine 1987). It follows that complete information about the effect of isotropic softening on the equilibrium of 2-D discs is already contained in $\mathscr{S}(|k|s)$, which in this context has the meaning of a reduction factor for the transformed surface density.

The relative quadratic deviations. The formulae for the angular speed $\Omega(R)$ and $\kappa(R)$ are of particular interest since these quantities also determine the stability and relaxation properties:

$$\Omega^2(R) = \frac{2\pi G}{R} \, \mathscr{H}_1 \left[\tilde{\Sigma}(k) \mathscr{S}(|k|s) \right](R), \tag{18}$$

$$\begin{aligned} \kappa^2(R) = \; & 2\pi G \, \mathscr{H}_0 \left[k \, \tilde{\Sigma}(k) \mathscr{S}(|k|s) \right](R) \\ & + \frac{4\pi G}{R} \, \mathscr{H}_1 \left[\tilde{\Sigma}(k) \mathscr{S}(|k|s) \right](R), \end{aligned} \tag{19}$$

$\tilde{\Sigma}(k)$ being an abbreviation for $\mathscr{H}_0[\Sigma(R)](k)$. The relative quadratic deviations of $\Omega(R)$ and $\kappa(R)$ from their Newtonian behaviours

$$\epsilon_g(R) = \frac{\left| g^2(R) - g_{\mathrm{N}}^2(R) \right|}{g_{\mathrm{N}}^2(R)} \quad (g = \Omega, \kappa) \tag{20}$$

depend on the model of mass distribution and on s/R_{d}, R_{d} being the disc scale length. In order to estimate the magnitude of these deviations, we can set $\mathscr{S} \sim 1 - |k|h$ and find that $\epsilon_g = \mathrm{O}(h/R_{\mathrm{d}}) \ll 1$, which is strictly valid for $R \gg h$ [the approximate formula for the circular speed is: $v_{\mathrm{c}}^2(R) \approx v_{\mathrm{cN}}^2(R) + 2\pi G R \Sigma'(R) h$]. More important are the deviations that result near the centre. They imply a change in the number and/or location of the inner Lindblad resonances, for a given pattern speed, together with larger natural scales for λ, c, s, h and t_{RW}. The contribution of a massive bulge to the rotation curve makes the system more robust against such modifications, but in certain respects this modelling is unclear and we are not yet in a position to draw quantitative conclusions (cf. Bertin 1996; Bertin & Lin 1996; Junqueira & Combes 1996, Sect. 2.2).

2.2. 3-D models with isotropic/anisotropic softening

2.2.1. 3D vs. 2D

The dynamics of 3-D discs with isotropic softened gravity is difficult to investigate because the effects of softening combine with those of vertical random motion in a complicated form. Nevertheless, we do in part understand how to benefit from the additional degree of freedom introduced into such models. A simple scale argument suggests that we should choose values of s sufficiently smaller than the Newtonian characteristic scale height, otherwise softening would significantly affect the vertical structure at equilibrium, i.e. *both* the mass distribution *and* the thickness scale. Likewise, the 2-D stability analysis suggests that in 3D we should choose $s \ll s_{\mathrm{safe}}$, otherwise softening would significantly interfere with the effect of thickness, as far as density waves are concerned. Note that choices of $s \geq s_{\mathrm{crit}}$ have the same consequences as in 2D, since the critical stability characteristics do not depend on the temperature anisotropy. We mention that the vertical structure at equilibrium and the stability of 3-D discs with Newtonian gravity have been investigated in previous papers (Romeo 1990, 1992; see also Paper I).

The 3-D Jeans problem with isotropic softened gravity can be solved by using the technique of Fourier transforms (see,

e.g., Sneddon 1972; Bracewell 1986). In Cartesian coordinates, this is the natural approach for factorizing the convolution in the Poisson equation and investigating the dynamical effects of softening, as Pfenniger & Friedli (1993) have previously emphasized. In the following discussion we concentrate on the reduction factor and compare the Jeans problem with the dynamics of discs. The reduction factor for the volume density can be calculated analytically from:

$$\mathscr{S}(|\boldsymbol{k}|s) = |\boldsymbol{k}| \, \mathscr{T}_{\mathrm{s}}[r \varphi_s(r)](|\boldsymbol{k}|), \tag{21}$$

where $\boldsymbol{k}$ is the wavevector of the perturbation and $\mathscr{T}_{\mathrm{s}}$ denotes the Fourier sine transform:

$$\mathscr{T}_{\mathrm{s}}[g(r)](|\boldsymbol{k}|) = \int_0^\infty g(r) \, \sin(|\boldsymbol{k}|r) \, \mathrm{d}r. \tag{22}$$

Equation (21) follows from the definition of $\mathscr{S}$ and the spherical symmetry of φ_s, which allows expressing the 3-D Fourier exponential transform in terms of $\mathscr{T}_{\mathrm{s}}$. Two alternative equations that are more convenient for numerical computation can be obtained by first singling out the Newtonian behaviour of $\varphi_s(r)$ at long distances, and then integrating by parts (the integrand can be split in two ways). As regards the magnitude of $\mathscr{S}(|\boldsymbol{k}|s)$, $\mathscr{S} = 1 - \mathrm{o}(|\boldsymbol{k}|s)$ at small $|\boldsymbol{k}|s$ and $\mathscr{S} \ll 1$ at large $|\boldsymbol{k}|s$. The stability properties are weakly affected by softening. In particular, significant deviations of the marginally stable wavelength λ_0 from the Jeans wavelength λ_{J} would occur for values of s comparable to λ_{J}. For example, in the case of Plummer softening this can be shown by using the simple numerical approximation $\lambda_0 \approx \lambda_{\mathrm{J}} + \frac{3}{2}s$ for $\frac{1}{6}\lambda_{\mathrm{J}} \lesssim s \lesssim \frac{2}{3}\lambda_{\mathrm{J}}$ [the analytical formula for $\mathscr{S}(|\boldsymbol{k}|s)$ is reported in Appendix A]. Weinberg (1993) has shown that in analogous models with Newtonian gravity the dominant source of noise is represented by fluctuations on scales of stability interest. This fact and our stability analysis suggest that the collective relaxation properties are also weakly affected by softening. Thus, there is a *sharp* contrast between the Jeans problem and the dynamics of discs: a flattened geometry strengthens the effects of softening, and rotation makes them critical for values of s that are an order of magnitude below λ_{T}.

2.2.2. Anisotropy vs. isotropy

The dynamical properties of 3-D discs are roughly decoupled parallel and perpendicular to the plane, and a satisfactory modelling with isotropic softening may impose significantly different requirements on s. Pfenniger & Friedli (1993) have discussed an ingenious way of coping with this difficulty, viz. to introduce a further degree of freedom into such models: softening anisotropy. We assume that the point-mass potential $-Gm\varphi(\boldsymbol{r})$ is of the form $\varphi(\boldsymbol{r}) = \varphi(R, |z|)$, and depends on the planar and vertical softening lengths $s_\parallel$ and $s_\perp$, respectively. The particular form in which softening anisotropy is implemented defines $s_\parallel$ and $s_\perp$, and specifies their meaning in the context of the dynamical requirements.
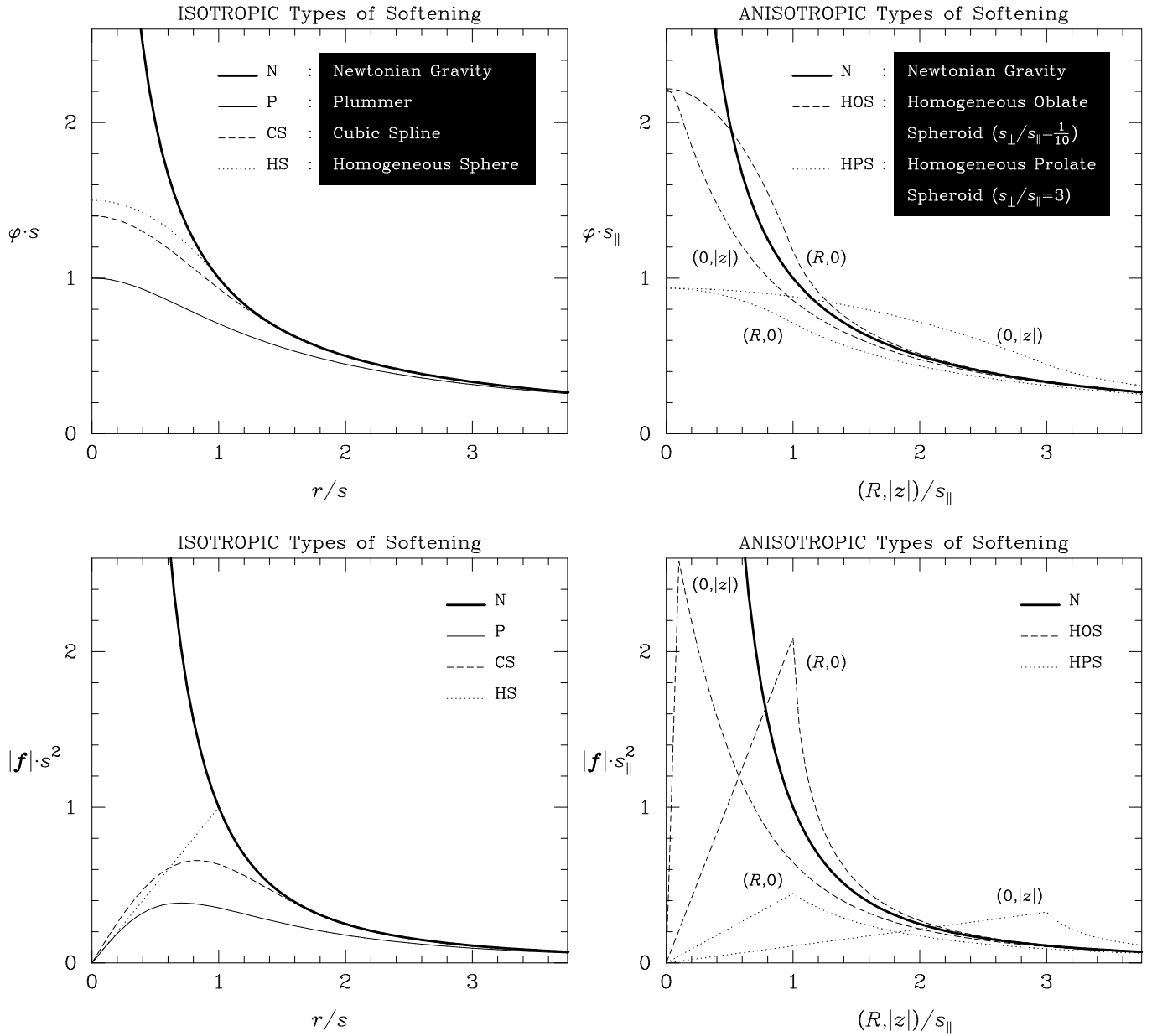
Fig. 2. The point-mass potential $-Gm\varphi(\boldsymbol{r})$ (top) and the magnitude of the force $Gm^2|\boldsymbol{f}|(\boldsymbol{r})$ (bottom) in isotropic (left) and anisotropic (right) types of softened gravity. In the isotropic types (discussed in Sect. 3.1) the gravitational interaction depends on the softening length s. In the anisotropic types (discussed in Sect. 3.2) the gravitational interaction depends on the planar and vertical softening semi-axes $s_\parallel$ and $s_\perp$, respectively. The anisotropic behaviour is only shown in the extreme cases $(R, |z| = 0)$ and $(R = 0, |z|)$, and is labelled accordingly

The 3-D Jeans problem shows the basic dynamical effects of softening anisotropy. The reduction factor may be evaluated from (cf. 2-D discs with isotropic softened gravity):

$$\mathscr{S}(k_\parallel, k_\perp) = (k_\parallel^2 + k_\perp^2)\, \mathscr{T}_c\left[\tilde{\varphi}(k_\parallel; |z|)\right](k_\perp), \qquad (23)$$

where $\tilde{\varphi}(k_\parallel; |z|)$ is an abbreviation for $\mathscr{H}_0[\varphi(R, |z|)](k_\parallel)$ and $\mathscr{T}_c$ denotes the Fourier cosine transform. This equation follows from the axial and planar symmetries of φ, which allow expressing the 3-D Fourier exponential transform in terms of $\mathscr{H}_0$ and $\mathscr{T}_c$. Supposing that $s_\parallel > s_\perp$, then we expect that

$\mathscr{S}(k_\parallel, 0) < \mathscr{S}(0, k_\perp)$ for $k_\parallel = k_\perp$, which means that the stability and collective relaxation properties are more affected parallel than perpendicular to the plane of reference.

3. Applications

3.1. Isotropic types of softening

As a first application of our method, we compare the dynamical effects of three isotropic types of softened gravity: Plummer softening (Aarseth 1963; Miller 1970), cubic-spline softening
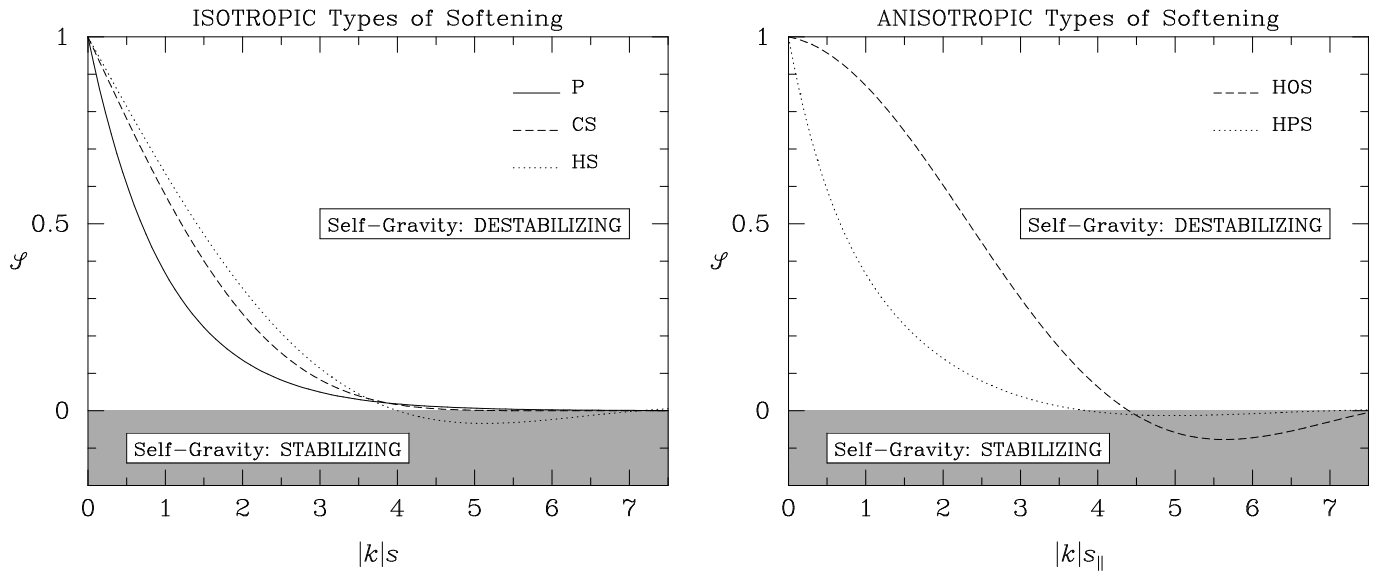
Fig. 3. The reduction factor $\mathscr{S}(k)$ of 2-D discs with isotropic (left) and anisotropic (right) types of softened gravity, k being the radial wavenumber of the perturbation. In addition, s is the softening length, $s_\parallel$ is the planar softening semi-axis, and the types of softened gravity are abbreviated as in Fig. 2. Also shown are the ranges in which the contribution of self-gravity to the dispersion relation is stabilizing and destabilizing. (In the case with Newtonian gravity $\mathscr{S} = 1$)

Table 1. Stability and relaxation characteristics of 2-D discs with isotropic (top) and anisotropic (bottom) types of softened gravity

Type of Softened Gravity	Abbr.	Softening Parameter					Related Quantities				
		η_{op1}[a]	η_{op}[b]	η_{op2}[a]	η_{safe}[c]	η_{crit}[d]	$\mathscr{C}$[e]	τ_{op}[f]	δ_{op}[g]	ζ/η[h]	$\bar\lambda_{\mathrm{crit}}$[i]
Plummer	P	0.03	0.12	0.25	0.20	0.37	1.70	0.05	0.39	1.00	0.37
Cubic Spline	CS	0.06	0.23	0.44	0.45	0.61	0.99	0.11	0.30	0.44	0.46
Homogeneous Sphere	HS	0.07	0.27	0.52	0.53	0.71	0.83	0.12	0.30	0.38	0.47
Homogeneous Oblate Spheroid [j]	HOS	0.18	0.55	0.94	——	1.21	0.44	0.32	——	0.04	0.61
Homogeneous Prolate Spheroid [j]	HPS	0.03	0.11	0.24	0.18	0.37	1.73	0.05	0.39	1.13	0.33

[a] Values corresponding to one half the optimal relaxation level.
[b] Optimal choice.
[c] Safety threshold for approximate physical consistency.
[d] Critical value.
[e] Correction factor for the Rybicki-White relaxation time.
[f] Optimal relaxation level.
[g] Temperature anisotropy corresponding to the stability threshold for the optimal value of the effective thickness parameter.
[h] Conversion factor, ζ being the effective thickness parameter (below the safety threshold for approximate physical consistency).
[i] Critical radial wavelength.
[j] HOS has $s_\perp/s_\parallel = \frac{1}{10}$ and HPS has $s_\perp/s_\parallel = 3$, where $s_\parallel$ and $s_\perp$ are the planar and vertical softening semi-axes, respectively, and $s_\parallel$ is regarded as the softening length of reference.

(Hernquist & Katz 1989) and homogeneous-sphere softening (Pfenniger & Friedli 1993); hereafter abbreviated to P, CS and HS, respectively. Each name means that the softened point-mass potential can be viewed as the Newtonian potential generated by a spherical mass distribution of that type (but the force is evaluated regarding the test particle as a point mass). In the following discussion we do not refer to this finite-sized particle interpretation of softening, unless otherwise specified. The behaviours of these types of softened gravity are shown in Fig. 2 (left).

In P the gravitational interaction is softened mainly at short distances and the Newtonian behaviour is recovered asymptotically, whereas in CS and HS softening is perfectly localized, i.e. beyond a certain cut-off distance the gravitational interaction is identically Newtonian. The form in which localization is implemented differs in the two types. In particular, CS has a rather soft cut-off at $r = 2s$, s being the nominal softening length, whereas HS has a sharper cut-off at $r = s$. The results of the dynamical comparison are presented in Fig. 3 (left) and
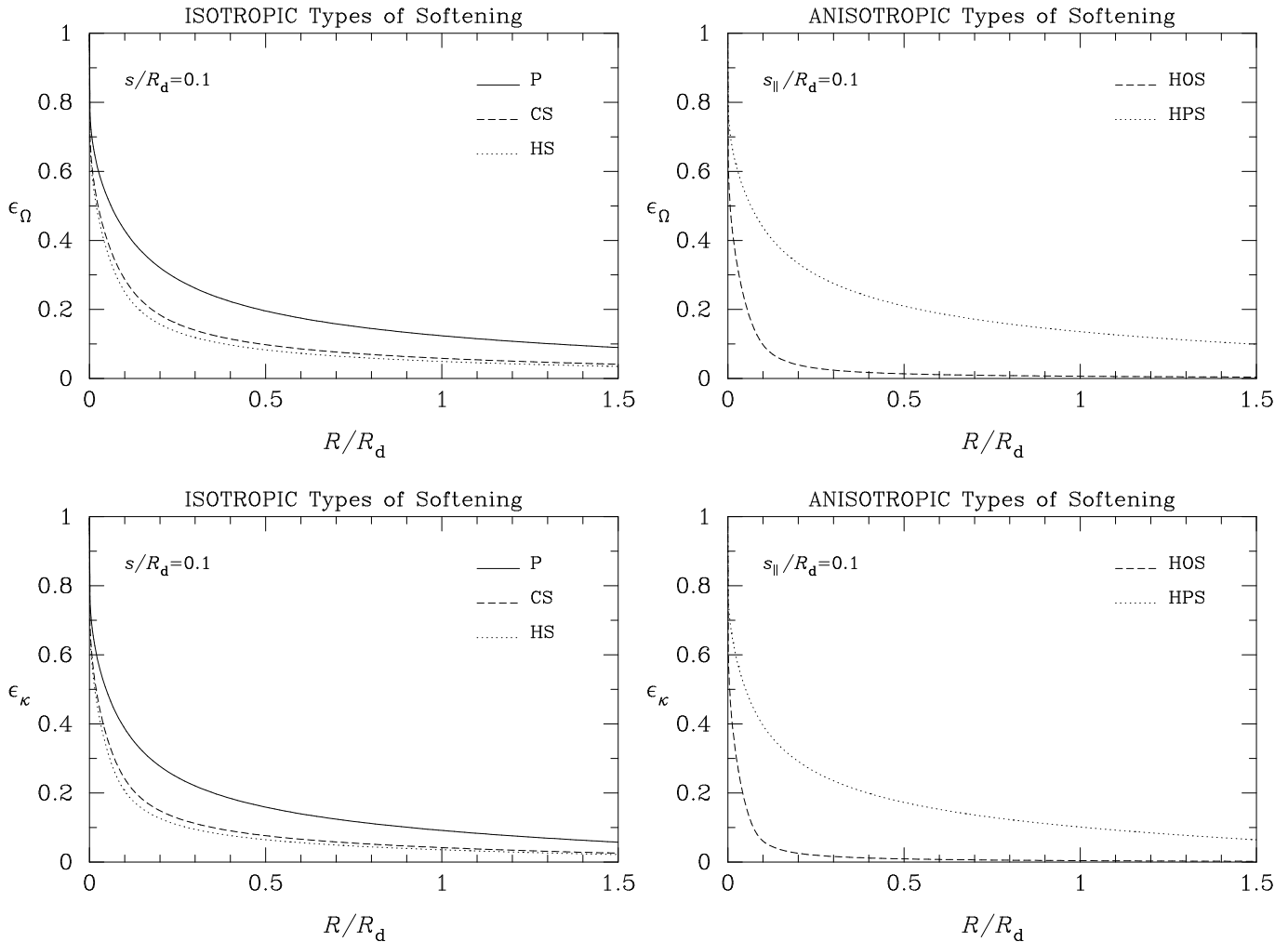
Fig. 4. The relative quadratic deviations $\epsilon_\Omega(R)$ (top) and $\epsilon_\kappa(R)$ (bottom) of 2-D exponential discs with isotropic (left) and anisotropic (right) types of softened gravity, where Ω is the angular speed, κ is the epicyclic frequency and the deviations are measured from their Newtonian behaviours. In addition, $R_{\mathrm d}$ is the disc scale length, s is the softening length, $s_\|$ is the planar softening semi-axis, and the types of softened gravity are abbreviated as in Fig. 2. (In the case with Newtonian gravity $\epsilon_\Omega = \epsilon_\kappa = 0$)

Table 1 (top), which are discussed below, and in Figs. 4 (left) and 5. Useful analytical formulae are reported in Appendix A.

Fig. 3 (left) shows that the effective scale height h varies significantly with softening type, but apart from that the stability properties are analogous on scales larger than $2h$. This can be shown by rescaling k in terms of h^{-1} and noting that $\mathscr{S}$ is similar in the three types for $|k|h \lesssim \frac{1}{2}$. For $|k|s \gtrsim 4$, $\mathscr{S}_{\mathrm{HS}}$ changes sign and starts to oscillate, in contrast to $\mathscr{S}_{\mathrm P}$. An analogous behaviour occurs in $\mathscr{S}_{\mathrm{CS}}$, but is less noticeable. Negative values of $\mathscr{S}$ mean that a given surface-density perturbation is in phase with the induced potential perturbation and, correspondingly, that the contribution of self-gravity to the dispersion relation is stabilizing. However, this feature does not affect the stability properties on scales comparable to the inverse of the typical radial wavenumber, since $\mathscr{S}$ changes sign well beyond the critical point $k_{\mathrm{crit}}s_{\mathrm{crit}}$ [cf. Table 1 (top)]. The related oscillations of $\mathscr{S}$ mean that in certain ranges of $|k|s$ noise is suppressed more effectively on larger than smaller scales, and correspond to os-

cillations of the short-wave branch of the dispersion relation. On the other hand, this feature has not significant consequences for the relaxation properties, because the corrected optimal relaxation level $\mathscr{C}\tau_{\mathrm{op}}$ is approximately the same as in P [cf. Table 1 (top)].

Table 1 (top) shows that the stability and relaxation characteristics vary significantly with softening type. The largest variations occur between HS and P, concern ζ/η and η_{safe}, and are up to a factor of 3. In contrast, the corrected optimal relaxation level $\mathscr{C}\tau_{\mathrm{op}}$, δ_{op} and $\bar\lambda_{\mathrm{crit}}$ remain approximately constant. The variations between HS and CS are within 20%.

3.2. Anisotropic types of softening

As a second application of our method, we consider an anisotropic generalization of HS, the family of homogeneous-ellipsoid softening (Pfenniger & Friedli 1993), and compare the dynamical effects of two representative spheroidal members:
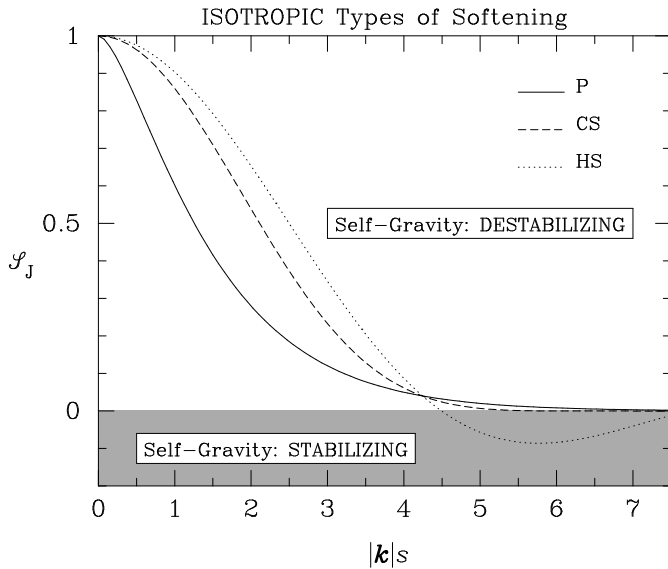
Fig. 5. The reduction factor $\mathscr{S}(|\boldsymbol{k}|s)$ for the 3-D Jeans problem with isotropic types of softened gravity, where $\boldsymbol{k}$ is the wavevector of the perturbation and s is the softening length. In addition, the types of softened gravity are abbreviated as in Fig. 2. Also shown are the ranges in which the contribution of self-gravity to the dispersion relation is stabilizing and destabilizing. (In the case with Newtonian gravity $\mathscr{S} = 1$)

one oblate with $s_\parallel : s_\perp = 10 : 1$, $s_\parallel$ and $s_\perp$ being the planar and vertical softening semi-axes, and the other prolate with $s_\parallel : s_\perp = 1 : 3$; hereafter abbreviated to HOS and HPS, respectively. Regarding $s_\parallel$ as the softening length of reference, $s_\perp/s_\parallel$ gives a measure of softening anisotropy. The behaviours of these types of softened gravity are shown in Fig. 2 (right). Anisotropy is implemented in a form consistent with the finite-sized particle interpretation of softening, i.e. through a spheroidal deformation of the field particle. This mainly corresponds to a spheroidal transformation of the surface on which the force peaks, but it also strongly influences the behaviour in the plane. In particular, the degree of softening localization, the sharpness and magnitude of the force peak differ from those in HS [cf. Fig. 2 (left)], and are higher in HOS than HPS. So a 2-D analysis is required even though the isotropic case has already been investigated. The results of the dynamical comparison are presented in Fig. 3 (right) and Table 1 (bottom), which are discussed below, and in Fig. 4 (right). The major points are then generalized in the final discussion. Useful analytical formulae are reported in Appendix A.

Fig. 3 (right) shows that, for $|k|s_\parallel \lesssim 2$, $\mathscr{S}_{\text{HOS}}$ is concave, in contrast to $\mathscr{S}_{\text{HPS}}$. The transition behaviour occurs in $\mathscr{S}_{\text{HS}}$ [cf. Fig. 3 (left)]. Concavity of $\mathscr{S}$ mainly means that softening has a stronger tendency to cause artificial stabilization for a given effective scale height h, for we know that the reduction factor of 3-D discs with Newtonian gravity is convex (cf. Paper I, Fig. 1). In fact, HOS does not mimic the effect of thickness for realistically large values of h, since the safety threshold for approximate physical consistency s_{safe} and the optimal value h_{op} are ill-defined [cf. Table 1 (bottom)]. Concavity of $\mathscr{S}$ also

means that softening causes a moderate degree of 'redshift'. For $|k|s_\parallel \gtrsim 4$, $\mathscr{S}_{\text{HOS}}$ and $\mathscr{S}_{\text{HPS}}$ become analogous to $\mathscr{S}_{\text{HS}}$, and analogous conclusions can be drawn concerning the stability and relaxation properties.

Table 1 (bottom) shows that the stability and relaxation characteristics differ considerably in the two types. The major qualitative differences concern η_{safe} and δ_{op}, and have been pointed out above [cf. discussion of Fig. 3 (right)]. Excluding ζ/η, which has a restricted range of applicability in HOS, the largest variation concerns τ_{op} and is beyond half an order of magnitude. In contrast, note the low sensitivity of the corrected optimal relaxation level $\mathscr{C}\tau_{\text{op}}$, which remains roughly constant.

Finally, instead of comparing those results with the isotropic case, let us clarify the dynamical relations between *all* the spheroidal members of the family of homogeneous-ellipsoid softening and the standard type of softened gravity [cf. Table 1 (top)].

1. A general feature of the spheroidal members is that h is determined by $s_\perp$ alone: $h = \frac{3}{8}s_\perp$. This is not intuitive since a more natural softening length in the plane is expected to be $s_\parallel$.
2. All the oblate members with $s_\perp/s_\parallel \lesssim \frac{3}{5}$ have an ill-defined s_{safe}, i.e. $s_{\text{safe}} \gtrsim s_{\text{crit}}$, and thus differ fundamentally from P (cf. HOS).
3. As $s_\perp/s_\parallel$ increases, such a difference becomes progressively less important (cf. HS and HPS). Indeed, the prolate member with $s_\perp/s_\parallel = \frac{8}{3}$, i.e. $h = s_\parallel$, turns out to be hardly distinguishable from P. (Values of $s_\perp/s_\parallel \gtrsim 2$–3 are not employed in simulations.)

4. Conclusions

Modelling gravity is a fundamental problem that must be tackled in N-body simulations of stellar systems, and satisfactory solutions require a deep understanding of the dynamical effects of softening. This problem has deserved special attention both in the past (e.g., Miller 1970, 1976) and in more recent times (e.g., Efstathiou et al. 1985; Hernquist & Katz 1989; Pfenniger & Friedli 1993). Viewed in this general perspective, our contribution has a threefold practical importance in addition to the points emphasized in Sect. 1.

1. The two present applications of our method reveal the dynamical differences between the most representative types of softened gravity: the isotropic P, CS and HS (abbreviated as in Sect. 3.1), and the anisotropic HOS and HPS (abbreviated as in Sect. 3.2). The major conclusions concerning their dynamical resolution, i.e. their faithfulness in simulating the Newtonian dynamics, are summarized below.
   (a) As regards the isotropic types, the dynamical resolution is comparable. This results from the fact that, even though the spatial resolution and the effectiveness in reducing noise differ significantly in P, CS and HS for the same nominal softening length s, those differences can largely be removed by considering a more appropriate softening length of reference.

(b) As regards the anisotropic types, the dynamical resolution is significantly coupled parallel and perpendicular to the plane. In the plane, it decreases in quality from HPS to HOS, and the transition occurs in the oblate members for a softening axial ratio $s_\perp/s_\parallel \sim \frac{3}{5}$ (HPS is dynamically similar to P). These disadvantages result from the finite-sized particle implementation of softening anisotropy. On the other hand, they have less importance than the advantage of introducing such a degree of freedom into 3-D simulations of disc galaxies, which has been emphasized by Pfenniger & Friedli (1993) and in our method.

(c) Last but not least, when employing these types of softened gravity in simulations of disc galaxies, we should recall that the dynamical resolution depends *critically* on two quantities: s, or $s_\parallel$ for a given $s_\perp/s_\parallel$, and the Safronov-Toomre parameter Q (cf. Paper I). The choice of s or $s_\parallel$ should be checked vs. the profiles of the characteristic values s_{op}, s_{safe} and s_{crit}, which are tabulated in the applications. The choice of Q should be checked vs. the profiles of the stability threshold $\bar{Q}$ and level Q_{eff}, which can be evaluated as is explained in the method.

2. Our method can be applied for testing new ideas about softening. There are two features that encourage such future applications.

(a) One is the *unified* approach adopted for investigating stability, relaxation and equilibrium. As a result, full information about the dynamical effects of softening is contained in a single quantity: the reduction factor $\mathscr{S}$.

(b) The other is the *modular* structure of the method. We describe step by step how to extract detailed information concerning the dynamical properties, starting from $\mathscr{S}$ and pointing out the quantities of major interest.

3. But our method can be applied in another, more fruitful, way: for developing new ideas about softening. Indeed, it opens a *direct* route to the discovery of optimal types of softened gravity for given dynamical requirements, and thus to the accomplishment of a physically consistent modelling even in the presence of a cold interstellar gaseous component. Such a future application will be the objective of a 'twin' paper.

Appendix A: useful analytical formulae for Sect. 3

$$\mathscr{S}_P(|k|s) = e^{-|k|s} ; \tag{A1}$$

$$(\zeta/\eta)_{P, CS, HS, HOS, HPS} = 1, \ \tfrac{31}{70}, \ \tfrac{3}{8}, \ \tfrac{3}{80}, \ \tfrac{9}{8} ; \tag{A2}$$

$$(\eta_{safe})_{P, CS, HS, HOS, HPS} = \tfrac{1}{5}, \ \tfrac{14}{31}, \ \tfrac{8}{15}, \ \text{---}, \ \tfrac{8}{45} ; \tag{A3}$$

$$(\eta_{crit})_P = \tfrac{1}{e} ; \tag{A4}$$

$$(\bar{\lambda}_{crit})_P = \tfrac{1}{e} ; \tag{A5}$$

$$(\mathscr{C})_{P, CS, HS} = \tfrac{16}{3\pi}, \ \tfrac{17\,325}{17\,504}, \ \tfrac{5}{6} ; \tag{A6}$$

$$\mathscr{S}_P(|k|s) = |k|s\,K_1(|k|s) , \tag{A7}$$

$$\mathscr{S}_{CS}(|k|s) = \frac{\sin^3(|k|s/2)}{(|k|s/2)^3} \, \mathscr{S}_{HS}(|k|s/2) , \tag{A8}$$

$$\mathscr{S}_{HS}(|k|s) = \frac{3\,[\sin(|k|s) - |k|s\,\cos(|k|s)]}{(|k|s)^3} , \tag{A9}$$

where K_ν denotes the modified Bessel function of the second kind and order ν (see, e.g., Abramowitz & Stegun 1972).

References

Aarseth S.J., 1963, MNRAS 126, 223

Abramowitz M., Stegun I.A., 1972, Handbook of Mathematical Functions – with Formulas, Graphs, and Mathematical Tables. Dover, New York

Bender C.M., Orszag S.A., 1978, Advanced Mathematical Methods for Scientists and Engineers. McGraw-Hill, Auckland

Bertin G., 1996, Spiral Structure in Galaxies: Competition and Cooperation of Gas and Stars. In: Block D.L., Greenberg J.M. (eds.) New Extragalactic Perspectives in the New South Africa. Kluwer, Dordrecht, p. 227

Bertin G., Lin C.C., 1996, Spiral Structure in Galaxies – A Density Wave Theory. MIT Press, Cambridge

Binney J., Tremaine S., 1987, Galactic Dynamics. Princeton University Press, Princeton

Bracewell R.N., 1986, The Fourier Transform and Its Applications. McGraw-Hill, New York

Byrd G., 1995, Tidal Perturbations, Gravitational Amplification, and Galaxy Spiral Arms. In: Hunter J.H. Jr., Wilson R.E. (eds.) Ann. N.Y. Acad. Sci. 773, Waves in Astrophysics. N.Y. Acad. Sci., N.Y., p. 302

Combes F., Debbasch F., Friedli D., Pfenniger D., 1990, A&A 233, 82

Efstathiou G., Davis M., Frenk C.S., White S.D.M., 1985, ApJS 57, 241

Farouki R.T., Salpeter E.E., 1994, ApJ 427, 676

Friedli D., 1994, private communication

Fulbright M.S., Benz W., Davies M.B., 1995, ApJ 440, 254

Gerber R.A., 1996, ApJ 466, 724

Goodman J., Heggie D.C., Hut P., 1993, ApJ 415, 715

Gradshteyn I.S., Ryzhik I.M., 1994, Table of Integrals, Series, and Products. Academic Press, Boston

Gueron S., 1994, J. Comput. Phys. 110, 164

Gurzadyan V.G., Pfenniger D. (Eds.), 1994, Ergodic Concepts in Stellar Dynamics. Springer-Verlag, Berlin

Hernquist L., Barnes J.E., 1990, ApJ 349, 562

Hernquist L., Katz N., 1989, ApJS 70, 419

Hernquist L., Ostriker J.P., 1992, ApJ 386, 375

Hockney R.W., Eastwood J.W., 1988, Computer Simulation Using Particles. Adam Hilger, Bristol

Junqueira S., Combes F., 1996, A&A 312, 703

Kandrup H.E., Smith H. Jr., Willmes D.E., 1992, ApJ 399, 627

Masset F., Tagger M., 1996, A&A 307, 21

Merritt D., 1996, AJ 111, 2462

Miller R.H., 1970, J. Comput. Phys. 6, 449

Miller R.H., 1976, J. Comput. Phys. 21, 400

Palouš J., Jungwiert B., Kopecký J., 1993, A&A 274, 189

Pfenniger D., 1993, Order and Chaos in N-Body Systems. In: Combes F., Athanassoula E. (eds.) N-Body Problems and Gravitational Dynamics. Observatoire de Paris, Paris, p. 1

Pfenniger D., Friedli D., 1993, A&A 270, 561

Romeo A.B., 1990, Stability and Secular Heating of Galactic Discs. PhD thesis, SISSA, Trieste, Italy

Romeo A.B., 1992, MNRAS 256, 307

Romeo A.B., 1994, A&A 286, 799 (Paper I)

Rybicki G.B., 1972, Relaxation Times in Strictly Disk Systems. In: Lecar M. (ed.) Proc. IAU Colloq. 10, Gravitational N-Body Problem. Reidel, Dordrecht, p. 22

Schroeder M.C., Comins N.F., 1989, ApJ 346, 108

Shapiro P.R., Martel H., Villumsen J.V., 1994, Adaptive Smoothed Particle Hydrodynamics and Galaxy Formation. In: Franco J., Lizano S., Aguilar L., Daltabuit E. (eds.) Numerical Simulations in Astrophysics. Cambridge University Press, Cambridge, p. 45

Shapiro P.R., Martel H., Villumsen J.V., Owen J.M., 1996, ApJS 103, 269

Shlosman I., Noguchi M., 1993, ApJ 414, 474

Shu F.H., 1968, The Dynamics and Large Scale Structure of Spiral Galaxies. PhD thesis, Harvard University, Cambridge, Massachusetts, USA

Sneddon I.N., 1972, The Use of Integral Transforms. McGraw-Hill, New York

Sommer-Larsen J., Vedel H., Hellsten U., 1997, ApJ (submitted)

Theis Ch., 1997, in preparation

Toomre A., 1963, ApJ 138, 385

Vandervoort P.O., 1970, ApJ 161, 87

van Veldhuizen M., Nieuwenhuizen R., Zijl W., 1994, J. Comput. Phys. 110, 196

Weinberg M.D., 1993, ApJ 410, 543

Weinberg M.D., 1996, ApJ 470, 715

White R.L., 1988, ApJ 330, 26

Zhang X., 1996, ApJ 457, 125